Nanoscale Advances

ROYAL SOCIETY OF CHEMISTRY

PAPER

View Article Online
View Journal | View Issue

Cite this: *Nanoscale Adv.*, 2021, **3**, 1443

Design of cross-linked polyisobutylene matrix for efficient encapsulation of quantum dots†

Anatol Prudnikau,‡[a] Dmitriy I. Shiman,‡[b] Evgenii Ksendzov,[ab] Jonathon Harwell,[c] Ekaterina A. Bolotina,[abe] Pavel A. Nikishau,[b] Sergei V. Kostjuk,[bde] Ifor D. W. Samuel[c] and Vladimir Lesnyak[a]

Photoluminescent quantum dots (QDs) are a prominent example of nanomaterials used in practical applications, especially in light-emitting and light-converting devices. Most of the current applications of QDs require formation of thin films or their incorporation in solid matrices. The choice of an appropriate host material capable of preventing QDs from degradation and developing a process of uniform incorporation of QDs in the matrix have become essential scientific and technological challenges. In this work, we developed a method of uniform incorporation of Cu–Zn–In–S (CZIS) QDs into a highly protective cross-linked polyisobutylene (PIB) matrix with high chemical resistance and low gas permeability. Our approach involves the synthesis of a methacrylate-terminated three-arm star-shaped PIB oligomeric precursor capable of quick formation of a robust 3D polymer network upon exposure to UV-light, as well as the design of a special ligand introducing short PIB chains onto the surface of the QDs, thus providing compatibility with the matrix. The obtained cross-linked QDs-in-polymer composites underwent a complex photostability test in air and under vacuum as well as a chemical stability test. These tests found that CZIS QDs in a cross-linked PIB matrix demonstrated excellent photo- and chemical stability when compared to identical QDs in widely used polyacrylate-based matrices. These results make the composites developed excellent materials for the fabrication of robust, stable and durable transparent light conversion layers.

Received 2nd December 2020
Accepted 19th January 2021

DOI: 10.1039/d0na01012j

rsc.li/nanoscale-advances

Introduction

Colloidal semiconductor nanocrystals (also known as quantum dots (QDs)) attract immense scientific and technological interest as promising materials for color conversion layers due to their exceptional optoelectronic properties such as broad-band absorption, precise size-dependent emission tunability, spectral purity and high photoluminescence (PL) efficiency.[1,2] These superior properties along with excellent solution processability make QDs suitable materials for a range of optoelectronic devices such as light emitting diodes (LEDs),[2–5] laser diodes,[6] displays,[7] solar cells,[8] and luminescent solar concentrators,[9] as well as emerging anticounterfeiting[10] and mechanoluminescence devices.[11] All these applications require processing of the QDs to make thin films, or their incorporation into solid matrices. The choice of an appropriate host material and optimization of transferring QDs from the solution to the solid matrix have become an important scientific and technological challenge. Although a number of attempts have been undertaken to find an optimal matrix for embedding QDs such as ionic crystals,[12–16] silica,[17] metal oxides,[18] or inorganic–organic hybrid materials,[19,20] polymers remain the most appropriate and promising matrices for this application.[21,22]

Polymers are attractive as host materials for QDs due to their low cost, simple processing and availability on an industrial scale. Dielectric polymers such as polydimethylsiloxane, polystyrene, and polyacrylates can be used as host materials for semiconductor nanocrystals due to their optical transparency in the visible region, high mechanical durability and extensive knowledge of their chemistry.[21,23–25] One of the most important parameters determining the use of a polymer as a host material for QDs is its flexibility. It should be noted that most popular polymer-based materials (polyacrylates and polystyrene derivatives) are rigid matrices, limiting their potential for

[a]*Physical Chemistry, TU Dresden, Zellescher Weg 19, 01069 Dresden, Germany. E-mail: vladimir.lesnyak1@tu-dresden.de*

[b]*Research Institute for Physical Chemical Problems of the Belarusian State University, Leningradskaya Str. 14, 220006 Minsk, Belarus. E-mail: kostjuks@bsu.by*

[c]*Organic Semiconductor Centre, SUPA, School of Physics and Astronomy, University of St. Andrews, North Haugh, St Andrews, Fife KY16 9SS, UK*

[d]*Institute for Regenerative Medicine, Sechenov First Moscow State Medical University, 119991 Moscow, Russia*

[e]*Department of Chemistry, Belarusian State University, Leningradskaya Str. 14, 220006 Minsk, Belarus*

† Electronic supplementary information (ESI) available: Description of the syntheses of SIBS, PLMA, tricumyl chloride and $FeCl_3 \cdot 1.4i\text{-PrOH}$; additional characterization; ^1H NMR spectra. TEM image of CZIS QDs; additional FTIR-spectra. See DOI: 10.1039/d0na01012j

‡ These authors contributed equally.

applications. Hence the practical interest is shifting towards flexible polymers, such as polyisobutylene (PIB), which exhibits excellent flexibility at ambient temperatures.[26]

There are various strategies for incorporation of colloidal QDs into polymer matrices without drastically changing their initial photophysical properties. One of the most widely used and simplest routes is the direct mixing of as-synthesized hydrophobic QDs with a solution of a polymer in nonpolar solvents, with subsequent evaporation of the solvent to create a solid matrix.[27,28] The other approach involves the dispersion of nanoparticles in monomers or prepolymerized oligomers and *in situ* polymerization for obtaining nanocomposites with embedded QDs.[22,24,29] Alternatively, nanoparticles can be synthesized directly in a preformed polymer matrix by decomposing suitable precursors under thermal treatment[30] or light irradiation.[31,32] Formation of both the nanocrystals and polymer matrix can occur at the same time.[22] Nevertheless, irrespective of the preparation method of polymer composites with embedded QDs, there are two critical issues which should be solved. The first problem is the inhomogeneous dispersion of QDs within polymer matrices, especially at high concentrations in the composite; and the second one is the insufficient stability of the obtained materials under working conditions.

The issue of poor compatibility between colloidal nanoparticles and polymers should be solved to avoid aggregation, which affects photophysical properties of QDs and leads to quenching of their PL and to formation of an opaque composite with strong turbidity. Colloidal QDs can be described as a complex material consisting of an inorganic core capped with a layer of organic molecules (ligands).[33] The ligands play a double role: on the one hand, they passivate dangling bonds on the QDs surface, on the other hand, they confer the compatibility of QDs with the surrounding media. This compatibility is very important as otherwise the QDs would be likely to aggregate, leading to a loss of quantum confinement and their distinctive properties. In particular, aggregation can greatly reduce PL efficiency. Modification of the surface through the ligand exchange process allows compatibility of colloidal QDs with different solvents and solid matrices to be achieved. For instance, originally hydrophobic CdSe/ZnS core/shell QDs were transferred to the aqueous phase by replacing initial ligands with mercaptosuccinic acid.[34] Functionalization of low-toxic Cu–Zn–In–S (CZIS) QDs with 4-vinylaniline and zinc methacrylate ensured their efficient copolymerization with styrene yielding QDs-in-polystyrene bulk composites with homogeneously distributed nanoparticles within the matrix with preserved high PL quantum yield (QY) of the QDs after the incorporation.[24]

The other serious obstacle for the commercialization of polymer composites with QDs is their insufficient stability under working conditions. As well known, oxygen and water can lead to QDs degradation and to the deterioration of their optical properties.[35] This is particularly relevant to Cd-free QDs, such as $CuInS_2$ and InP which typically demonstrate lower stability than cadmium chalcogenide-based QDs.[35] The most widely used approach to enhance stability of QDs is overcoating them with an epitaxial shell consisting of a wider band gap semiconductor material. In the case of $CuInS_2$ or CZIS, zinc sulfide is the most suitable candidate for the shell growth due to its low toxicity, high stability, and small crystal lattice mismatch.[36,37] Despite the fact that the shell confines excitons to the core, removes surface defects and protects the core from interaction with the environment,[33] this approach is limited since increasing the shell thickness can lead to deterioration of their PL properties due to crystalline mismatch at the core/shell interface inducing significant lattice strain that in turn leads to formation of crystal lattice defects.[38] The other approach to enhance the stability of QDs in solid composites is using host materials with low gas permeability and high chemical stability which allow for protecting QDs from oxygen and moisture even under harsh operating conditions.[27] Among flexible polymers (elastomers) suitable as a host material for QDs three main classes can be distinguished: silicones, polyurethanes and rubbers with hydrocarbon main chain. The first two classes are characterized by a very high gas permeability (5.86×10^{-15} m^2 s^{-1} Pa^{-1} and 8.93×10^{-15} m^2 s^{-1} Pa^{-1} respectively)[39,40] and are unable to protect QDs during operation. Among rubbers, butyl rubber (copolymer of isobutylene (98–99%) and isoprene (1–2%)) has the lowest gas permeability (4.29×10^{-17} m^2 s^{-1} Pa^{-1}).[39] In addition to low gas permeability, commercial butyl rubber has a vapor permeability 4.79×10^{-19} to 1.16×10^{-18} m^2 s^{-1} Pa^{-1} lower than most plastics ($0.48–3.34 \times 10^{-18}$ m^2 s^{-1} Pa^{-1}).[41] Furthermore, it possesses high chemical stability and retains high elastic properties at low temperatures ($T_g = -64$ °C).[42] Banerjee *et al.* and Bag *et al.* recently showed that compared to commercial butyl rubber, the cross-linked PIB-based star-shaped polymers exhibit better barrier properties, in particular, oxygen permeability of only 4.07×10^{-18} m^2 s^{-1} Pa^{-1} and moisture permeability of 9.86×10^{-17} m^2 s^{-1} Pa^{-1}, which are highly beneficial for encapsulation of flexible organic solar cells.[43,44]

In our previous work, we developed oxygen- and moisture-proof polymer matrices based on PIB for the encapsulation of colloidal semiconductor nanocrystals with different composition and dimensionality.[27] Since pure PIB is a soft polymer, we synthesized a block-copolymer of isobutylene with styrene poly(styrene-*block*-isobutylene-*block*-styrene) (SIBS) to improve mechanical properties of the composites. The nanocrystals were functionalized with a specially designed ligand, containing a short-chain PIB and anchor amino group, which provides excellent compatibility between nanocrystals and PIB-based matrices. It was also shown that semiconductor nanocrystals in PIB-based matrices demonstrated enhanced photo- and chemical stability.

In this work, we report a design principle of the QDs-in-polymer composite, which enables photoluminescent QDs to be incorporated in a highly protective cross-linked matrix without changing their optical properties. We synthesized a methacrylate-terminated three-arm star-shaped PIB precursor (PIB-MA) capable of fast hardening under the UV-light, forming a robust cross-linked polymer network. Using this approach, we solve the problem of the PIB softness and enhance the protective properties of the matrix. To test the encapsulation ability of cross-linked PIB-MA we used CZIS QDs, for which a special

procedure for the modification of their surface was developed to uniformly disperse embedded QDs in PIB-based matrices. The mixture of CZIS QDs and PIB-MA may be considered as a colloidal solution that can be rapidly transformed into the transparent solid bulk composite with complete preservation of the optical properties of the CZIS QDs after encapsulation. The cross-linked composites obtained have excellent photo- and chemical stability of the embedded QDs in comparison to the composites with poly(lauryl methacrylate) (PLMA). Our results show that cross-linked PIB is a promising material for fabrication of robust, durable and stable transparent composites which may be used as color conversion layers in displays or luminescent solar concentrators.

Experimental section

Chemicals

1,2-Ethanedithiol (≥98%), ethanol (99.5%), *n*-heptane (≥98%), anhydrous Na_2SO_4 (≥99%), dichloromethane (≥99.8%), *n*-hexane (≥95%), phenol (≥99%), hydrochloric acid (37%), indium(III) acetate ($In(OAc)_3$, 99.99%), 1-dodecanethiol (DDT, ≥98%), chloroform (≥99%), toluene (≥99.8%), trioctylamine (98%), 1-pentanethiol (98%), 1-octadecene (ODE, 90%), tetrahydrofuran (THF, >99.9 for HPLC), silica gel 60 (0.063–0.2 mm, for column chromatography) and ammonia solution (25%) were purchased from Sigma–Aldrich. Isobutylene (99%, Sigma–Aldrich) was dried in the gaseous state by passing through in-line gas-purifier packed with BaO/Drierite and then condensed in a receiver flask at −40 °C. Methanol (≥99.9%) and potassium hydroxide (KOH, analytical reagent grade) were purchased from Fisher Chemical. Polyisobutylene Glissopal® $M_n = 1000$ g mol^{-1} was purchased form BASF. Pyridine (≥99%) was purchased from Roth. Oleylamine (OlAm, 80–90%) was purchased from Acros. Isopropanol (HPLC grade) and acetonitrile (HPLC grade) were purchased from VWR Chemicals. Zinc 2-ethylhexanoate (*ca.* 80% in mineral spirits (17–19% Zn)) was purchased from Alfa Aesar. Methacryloyl chloride was purchased from Abcr. Pyridine and methacryloyl chloride were distilled right before using. Azobisisobutyronitrile (AIBN) (98%, Sigma-Aldrich) was recrystallized from ethanol. All other chemicals were used as received.

Synthesis of ((2-mercaptoethyl)thio)polyisobutylene (PIB-SH)

PIB-SH was synthesized according to the described method by reaction of PIB (Glissopal® 1000) with 1,2-ethanedithiol.[45] First, the mixture of 2 g of PIB (2 mmol) and 32.8 mg of AIBN (0.2 mmol) was degassed under vacuum and dissolved in 14 mL of *n*-heptane. Afterwards, 14 mL of dry ethanol and 0.33 mL of 1,2-ethanedithiol were added to the solution. The mixture was again degassed by three freeze–pump–thaw cycles followed by stirring under UV-light (365 nm) at room temperature for 8 hours. Thereafter the reaction mixture was diluted with 110 mL of *n*-heptane followed by addition of 10 mL of deionized water. *n*-Heptane phase was separated and washed three times with 50 mL portions of 90% ethanol and dried under anhydrous Na_2SO_4. The final product was obtained after evaporation of the solvent under reduced pressure.

Synthesis of three-arm star-shaped PIB

5 mL of 0.22 M $FeCl_3 \cdot 1.4$i-PrOH solution in CH_2Cl_2 were added to a mixture of 4.1 g of isobutylene (73.2 mmol), 32.5 mL of *n*-hexane, 16.5 mL of CH_2Cl_2, and 0.415 g of tricumyl chloride (1.35 mmol, synthesized as described in ref. 46) at −80 °C. After 50 seconds of stirring, the reaction mixture was poured into ethanol. The resulting precipitate of PIB was dissolved in 20 mL of *n*-hexane. Then the solution was centrifuged at 3000 rpm for 5 min to remove insoluble products and filtered through silica. The clear solution was mixed with 100 mL of methanol resulting in flocculation of PIB with its subsequent drying in vacuum at 40 °C.

Synthesis of hydroxyl-terminated three-arm star-shaped PIB

The synthesis is based on Friedel–Crafts alkylation of phenol by highly reactive three-arm PIB using the procedure described in ref. 47. Briefly, a flask for the synthesis was first degassed under vacuum and filled with argon thrice. Then 0.333 g of PIB ($M_n =$ 3500 g mol^{-1}, 0.095 mmol) were dissolved in 2.02 mL of 1.5 M phenol solution (3.03 mmol) in dichloromethane, followed by cooling down the solution to 0 °C and adding 0.025 mL of 98% sulfuric acid (0.14 mmol). Reaction was conducted at 0–20 °C for 36 hours upon stirring and then quenched by adding 2 mL of 25% solution of ammonia in water. Product was purified by filtration of solution in dichloromethane and its precipitation into ethanol. Pure polymer was dried under vacuum at 40 °C.

Synthesis of methacrylate-terminated three-arm star-shaped PIB (PIB-MA)

PIB-MA was synthesized according to the modified method[42] by acylation of hydroxyl-terminated PIB with methacryloyl chloride in the presence of pyridine. Briefly, 0.258 g of hydroxyl-terminated PIB (M_n = 4000 g mol^{-1}, 64.5 μmol) were dissolved in 0.7 mL of dichloromethane in thrice degassed and filled with argon flask. After adding 22.4 μL of pyridine (0.278 mmol), the mixture was cooled to 0 °C followed by addition of 27 μL of methacryloyl chloride (0.278 mmol). Synthesis was conducted at 0 °C for 1 hour upon stirring and then at room temperature for 48 hours. Product was purified by consequent washing of its solution in 50 mL of dichloromethane consequently by 2 M hydrochloric acid, 3% potassium hydroxide and distilled water. Pure sample was dried under vacuum at 20 °C.

Synthesis of CZIS gradient QDs

CZIS QDs were synthesized according to previously reported procedure[48] with slight modifications using a standard Schlenk line technique. Briefly, 466 mg of $In(OAc)_3$ (1.6 mmol), 6 mL of OlAm and 32 mL of ODE were loaded into a 100 mL three-neck flask and degassed under vacuum for 15 min at room temperature. Then the flask was filled with argon and the mixture was heated up to 150 °C until $In(OAc)_3$ was fully dissolved forming slightly opalescent solution. Then the mixture was cooled down

to room temperature and 25.6 mg of sulfur powder dissolved in 1 mL of OlAm by ultrasonication was added. The reaction system was degassed again for 15 min, filled with argon and heated up to 160 °C (20–25 °C per min). At 120 °C a suspension of 30.4 mg (0.16 mmol) of CuI in 2 mL of DDT was injected into the flask. At 160 °C the heating was stopped, and the reaction mixture cooled down to room temperature followed by the addition of 1.52 mL of the solution of zinc 2-ethylhexanoate in mineral spirits. The reaction mixture was degassed to remove mineral spirits, heated up to 290 °C and kept at this temperature for 20–30 min for incorporation of Zn atoms into $CuInS_2$ nanocrystals that was accompanied by a blue shift of the PL maximum to 610–620 nm. Then, the reaction mixture was allowed to cool down to room temperature by removing the heating mantel. The QDs were precipitated by addition of an isopropanol–methanol (10 : 1, v/v) mixture with subsequent centrifugation. The precipitate was dissolved in 5 mL of chloroform and precipitated by acetonitrile followed by centrifugation. The last procedure was repeated thrice and then supernatant was discarded and precipitate was dispersed in 3.5 mL of toluene.

Surface modification of CZIS QDs

To functionalize the QDs with PIB-SH, 300 μL of the stock solution of CZIS QDs were diluted with 1.2 mL of toluene. Then 670 μL of 5% solution of PIB-SH in toluene and 300 μL of 0.045 M solution of trioctylamine in toluene were added. The mixture was stirred overnight at room temperature. Then the QDs were precipitated by adding acetonitrile and subsequent centrifugation. To remove unbound ligands, QDs were additionally thoroughly purified three times using toluene and acetonitrile as a solvent and nonsolvent, respectively. The purified QDs were dispersed in 1.5 mL of toluene for further use in the preparation of the composites.

For the treatment of the CZIS QDs with the mixture of 1-pentanethiol and DDT we employed the same procedure as described above, but 300 μL of 0.045 M solution of 1-pentanethiol and 300 μL of 0.045 M solution of DDT in toluene were used instead of PIB-SH.

Films deposition

0.2 mL of the solution of surface-modified CZIS QDs obtained as described above were mixed with 1.87 mL of 0.83% wt. solution of the polymer (PIB-MA, SIBS, or PLMA) in toluene. The prepared solution was sprayed on the glass substrates with the size of 1 × 1 cm using the ultrasonic spray-coating technique (ultrasonic spray coater ND-SP from Nadetech Innovations). The deposition of all films was carried out in 20 layers, since using a multilayer deposition and diluted solutions of polymer resulted in a more homogenous coating.

Films cross-linking

PIB-MA films with embedded CZIS QDs were placed in a nitrogen-filled glovebox and were exposed to 365 nm UV-lamp (6 W, UVL-56 from Analytik Jena) for 1 hour at 5 cm distance.

Characterization

Absorption spectra were acquired with a Cary 60 spectrophotometer (Varian). PL spectra were obtained using a Fluoromax-4 (Horiba Jobin Yvon, Inc.) spectrofluorometer with the excitation wavelength set at 435 nm. Absolute PLQYs of liquid samples were determined employing a Fluorolog-3 spectrofluorometer equipped with a Quanta-ϕ integrating sphere (Horiba Jobin Yvon, Inc.). Absolute PLQYs of QDs-in-polymer composites were measured in ambient conditions using a Hamamatsu Photonics Absolute quantum yield integrating sphere and spectrometer setup (C9920-02). The samples were excited with 450 nm light from a monochromated xenon lamp source, and the PL was collected from the integrating sphere using a fibre coupled PMA-12 (C10027-01) spectrometer.

Fourier-transform infrared (FTIR) spectroscopy

The measurements were performed on a Nicolet 8700 FTIR spectrometer using the attenuated total reflectance (ATR) method. After ligand exchange CZIS QDs were purified through precipitation and redispersion (six times) using chloroform and acetonitrile as solvent and nonsolvent, respectively. After the final precipitation, QDs dried under vacuum for five hours, the obtained powder was ground and placed onto the ATR crystal.

Photostability test

The photostability of the samples was tested using a home-built setup schematically shown in Fig. SI1 in the ESI,† where the samples were exposed to high intensity excitation light from a 42 mW helium–cadmium (HeCd) laser with an emission wavelength of 442 nm and a beam diameter of 1 mm. After ensuring that the input excitation was stable, the PL from the sample was collected by a fiber bundle held at a fixed distance from the sample and its spectrum and intensity measured by an Andor CCD spectrograph. PL spectra of the sample were repeatedly taken at 5 second intervals under constant excitation to produce a kinetic series of the PL spectrum *vs.* time under these conditions. The PL spectrum (minus the background and scattered laser light) of each measurement was then integrated to produce a graph of integrated PL counts *vs.* time, which was then normalized to provide a measure of the relative change in PL *vs.* time under the photodegradation conditions. For samples measured under vacuum, an identical setup was used, with the exception that the samples were placed in an Oxford instruments cryostat kept at room temperature and pumped down to a pressure of roughly 10^{-6} mbar. The samples were measured and excited through optical windows in the cryostat, and samples were left overnight under high vacuum prior to measurement to ensure outgassing of any adsorbed air.

Results and discussion

Methacrylate-terminated three-arm star-shaped PIB with two different molar weights (M_n (NMR) = 4200 and 5600 g mol^{-1}, respectively) was used as an oligomeric precursor to form a cross-linked polymer matrix with embedded Cd-free QDs. As

illustrated in Fig. 1a, the synthesis of PIB-MA includes three main steps. The first step consists of the living cationic polymerization of isobutylene in the presence of a trifunctional initiator (1,3,5-tris(2-chloropropan-2-yl)benzene (tricumyl chloride)) and a complex of iron chloride with 1.4 equivalents of isopropyl alcohol as a co-initiator in dried *n*-hexane/dichloromethane mixture at low temperature. We demonstrated the higher activity of the complex $FeCl_3 \cdot 1.4$i-PrOH

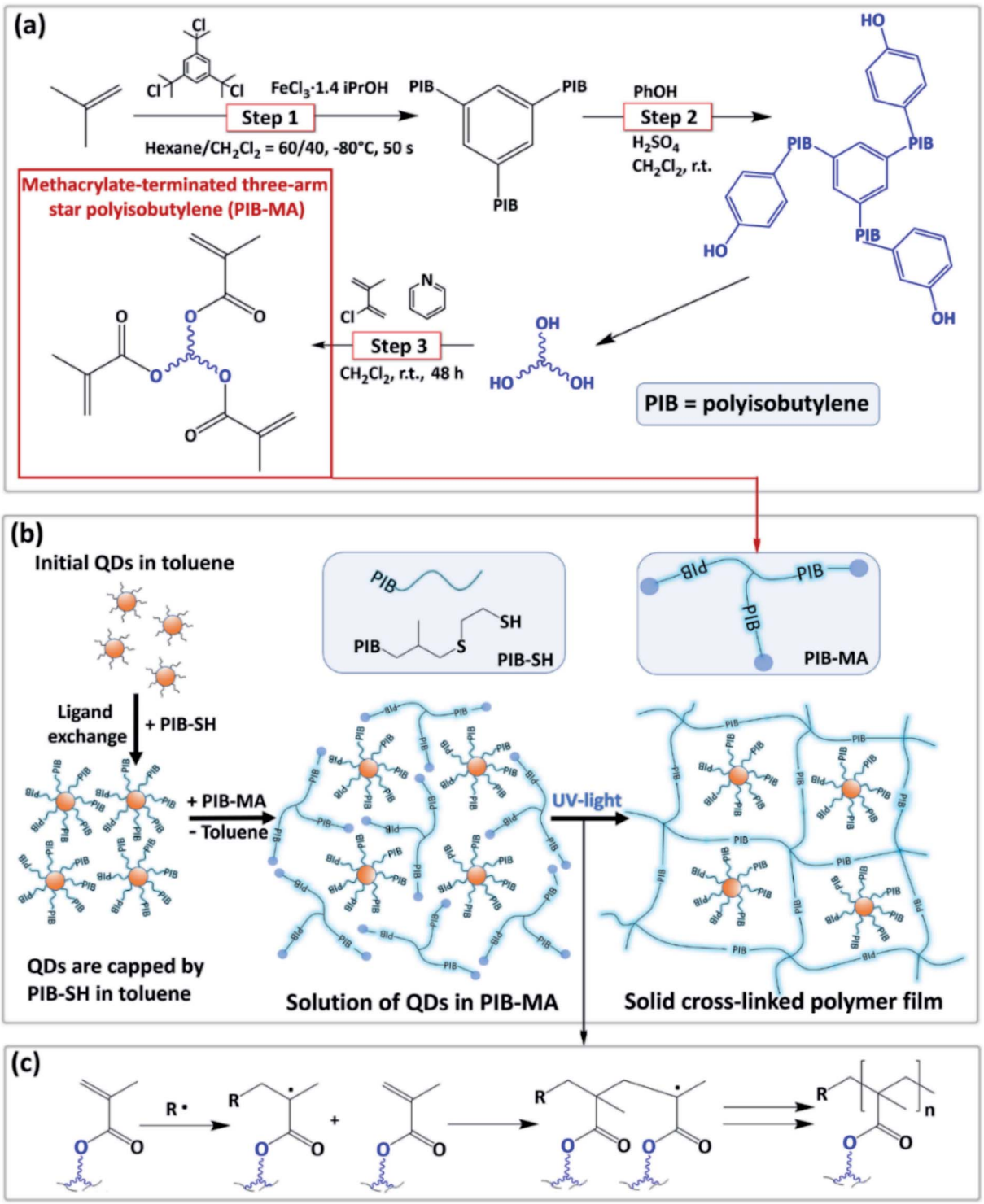

Fig. 1 Scheme of the synthesis of PIB-MA including the synthesis of three arm star-shaped PIB (step 1) and its modification *via* consecutive alkylation of phenol (step 2) followed by methacrylation (step 3) (a). Scheme of the preparation of cross-linked PIB with embedded QDs including modification of the QD surface with PIB-SH, dispersion of obtained QDs in PIB-MA and its cross-linking under UV irradiation (b). Scheme of cross-linking of PIB-MA (c).

developed by Wu and co-workers[49,50] in comparison with $TiCl_4$ in the polymerization of isobutylene in the presence of tricumyl chloride as an initiator. Addition of $FeCl_3 \cdot 1.4$i-PrOH resulted in a complete conversion of the monomer into PIB with a low polydispersity ($M_w/M_n = 1.13$) in less than a minute reaction time. At the same time, employing a more traditional initiating system based on $TiCl_4$ requires longer reaction times of up to 45 min and the presence of amines as proton traps.[42] According to the results of ^{1}H NMR spectroscopy (see Fig. SI2†), the obtained oligomer is terminated with *exo*-olefin (35 mol%) and tertiary chloride (65 mol%) end groups, which are active in Friedel–Crafts alkylation. The next step was the alkylation of phenol by synthesized three-arm star-shaped PIB in the presence of sulfuric acid. According to the ^{1}H NMR spectrum (see Fig. SI3†), the alkylation process led to conversion of tertiary chloride and *exo*-olefin groups of three-arm star-shaped PIB with formation of only *para*-alkylated phenol. The final step was acylation with conversion of OH-terminal groups into methacrylate groups. The molecular structure of obtained PIB-MA was confirmed by ^{1}H NMR analysis (see Fig. SI4†). PIB-MA with M_n (NMR) = 4200 or 5600 g mol^{-1} is a viscous colorless liquid readily soluble in organic solvents such as toluene or chloroform.

The obtained oligomeric precursors PIB-MA with different molecular weights of $M_n = 4200$ and 5600 g mol^{-1} were used for fabrication of cross-linked QDs-in-polymer composites. In addition to the synthesis of appropriate QDs and PIB-MA, the procedure of the composite preparation included three main steps, which are schematically shown in Fig. 1b. First, the surface modification of the as-synthesized CZIS QDs was performed through the ligand exchange to achieve high compatibility between the QDs and PIB-MA. For this procedure we synthesized ((2-mercaptoethyl)thio)PIB (PIB-SH) with a molecular weight of 1000 g mol^{-1}, which played a role of a specially designed oligomeric ligand containing thiol anchor group and PIB chain (see Fig. SI5†). As previously reported, the nanocrystals capped by the ligand with hydrocarbon chains with the same chemical structure as the polymer matrix form homogeneous composites.[27,51] On the other hand, thiols are suitable capping agents for most semiconductor nanoparticles due to a strong affinity of the –SH group to metal atoms on the nanocrystal surface. Then, modified QDs were dissolved in a toluene solution of PIB-MA and deposited on the glass substrate using an ultrasonic spray-coater. The parameters of the spray-coater were adjusted to realize efficient toluene evaporation during the film deposition. In the final stage, mixture of QDs and PIB-MA on the glass substrate was exposed to UV-light in an inert atmosphere resulting in cross-linking of PIB-MA through radical polymerization of methacrylate end groups (see Fig. 1c) and in the formation of a solid polymer network with embedded QDs. Thereafter we tested photo- and chemical stability of the composites of CZIS QDs with the obtained cross-linked polymers based on PIB-MA with two different molecular weights, comparing them with the other polymers such as SIBS and PLMA.

To test PIB-MA as a host material for fabrication of QDs-in-polymer composites we synthesized CZIS QDs using the modified protocol described in ref. 48. This protocol includes a multi-step approach in which In-rich CIS QDs are synthesized first in the presence of DDT and then are treated with a large excess of Zn-precursor at high temperature to obtain CZIS quaternary nanocrystals with gradient core/shell structure. Thus synthesized CZIS QDs with the size of approx. 2.6 nm (see Fig. SI6†) demonstrated typical optical properties of I–III–VI semiconductor nanocrystals,[52] such as absorption without a distinct excitonic feature, broad PL spectrum and large Stokes shift. They had relatively high PLQY of 52% with the PL maximum at 617 nm (Fig. 2a). These QDs are an excellent candidate for testing host polymer materials for a number of reasons. First of all, the I–III–VI group-based QDs along with InP QDs are the most promising Cd- and Pb-free materials for fabrication of solid-state optoelectronic devices with PL in the visible region.[5,53,54] Second, a gradient core/shell architecture of the synthesized CZIS QDs allows conducting their purification and surface modification without changing their optical properties. As has been shown, the photostability of CIS QDs can be enhanced through increasing ZnS shell thickness.[55] Nevertheless, since our main goal was to investigate the encapsulation properties of the cross-linked PIB in comparison with other polymers, we deliberately produced CZIS QDs with a relatively thin shell to observe changes in their optical properties on a short timescale.

The surface modification of CZIS QDs is necessary to provide compatibility with PIB-MA ensuring their homogeneous dispersion. Even though as-synthesized hydrophobic CZIS QDs can easily be mixed with solutions of PIB-MA in toluene, subsequent evaporation of the solvent leads to imminent aggregation of nanocrystals resulting in a turbid composite. Thus, to improve compatibility between PIB-MA and CZIS QDs, as-synthesized nanoparticles underwent the surface modification through the ligand exchange. The approach that we used for the synthesis of CZIS QDs, like most known recipes,[56] involves the addition of an excess of DDT to adjust the relative reactivity of copper and indium precursors that leads to the formation of DDT-capped CZIS QDs. Since thiols were found to have a high affinity to metal atoms on the nanocrystal surface, it is particularly challenging to replace them with other ligands such as carboxylates or amines.[52] At the same time, partial exchange of initial thiol for the desired thiol is possible despite low lability of the outgoing ligand. Thus, Lefrançois and co-authors have shown that treatment of DDT-capped $CuInS_2$ QDs with 1,2-ethylhexanethiol in chloroform at room temperature resulted in the replacement of approx. 70% of DDT with 1,2-ethylhexanethiol.[57]

To facilitate the replacement of DDT with PIB-SH, the ligand exchange was performed in the presence of trioctylamine, since the addition of a base accelerates deprotonation of thiol groups forming thiolate anions.[58,59] After treatment of CZIS QDs with PIB-SH and thorough purification of the modified QDs they formed a homogeneous dispersion in PIB-MA without any apparent aggregation or phase separation that evidences a presence of PIB chains on the QDs surface. Additional evidence provided results of the FTIR spectroscopy presented in Fig. 2b and SI7.† To remove the unbound ligands, the QDs were

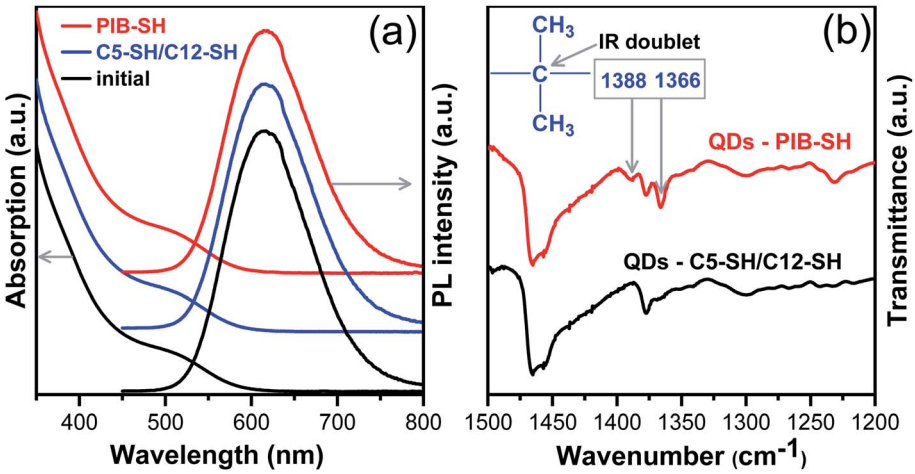

Fig. 2 Absorption and PL spectra of CZIS QDs in toluene before and after the treatment with thiols (a). The spectra are offset vertically for clarity. FTIR spectra of as-synthesized and capped with PIB-SH CZIS QDs (b).

subjected to six times precipitation using chloroform and acetonitrile as a solvent and an antisolvent, respectively. In the FTIR spectrum of modified CZIS QDs the characteristic doublet at 1388 and 1366 cm^{-1} appeared clearly indicating PIB-SH attached to the QDs surface. This doublet is a result of the coupling between the symmetric bending modes of the two methyl groups in R–C$(CH_3)_2$–R moiety.[60] In addition to FTIR analysis, the ^{1}H NMR spectrum of extensively purified CZIS QDs unambiguously demonstrates PIB-SH resonances after the ligand exchange (see Fig. SI8†). As one can see in Fig. 2a, after the treatment with PIB-SH there were no changes in spectra revealing complete preservation of optical properties of the initial QDs. In addition, there was no remarkable change in PLQY (52% before and 54% after the treatment).

As-synthesized CZIS QDs with DDT molecules on the surface can be easily embedded in PLMA matrix forming transparent composite due to a good compatibility between lauryl-chains of PLMA and DDT. Nevertheless, for producing QDs-in-PLMA composite the QDs were modified with a mixture of 1-pentanethiol and DDT in the presence of trioctylamine using the same protocol as for the treatment of the QDs with PIB-SH. We assumed that the presence of alkylthiols with different chain lengths on the QDs surface may lead to the formation of a less dense ligand shell resulting in more efficient interpenetration of the lauryl chains of PLMA and the hydrocarbon surface ligands. In addition, since QDs-in-PLMA composite was used as a reference sample for testing encapsulation properties of cross-linked PIB-MA matrix, it was particularly important that QDs in the case of all composites were prepared under the same conditions including purification and post-synthetic treatment steps. As expected, after the treatment of CZIS QDs with a mixture of alkylthiols we did not observe any changes in their PL and absorption spectra (see Fig. 2b), PLQY values (52%), and FTIR-spectra (see Fig. SI7†).

After the ligand exchange and the thorough purification, CZIS QDs with tethered PIB-SH were dispersed in the solution of PIB-MA in toluene. The obtained solutions were sprayed on glass substrates using an ultrasonic spray-coater. Since PIB-MA oligomers (both M_n = 4200 and 5600 g mol^{-1}) are viscous liquids at room temperature, the mixture of PIB-SH-capped QDs with PIB-MA on the substrate after toluene evaporation can be considered as a colloidal solution. The resulting "liquid" films were then converted into solid cross-linked polymer films (CL-PIB4K and CL-PIB5K for cross-linked PIB-MA with M_n 4200 and 5600 g mol^{-1}, respectively) by exposing the samples to the UV-light in the nitrogen filled glovebox. After the polymerization we registered disappearance of the double bond of acrylate group in FTIR-spectrum of QDs-in-PIB-MA film (see Fig. SI9†). The cross-linked QDs-in-polymer composites obtained were found to be resistant to a prolonged soaking in chloroform for at least one month (see Fig. SI10†), which evidences the formation of robust cross-linked polymer network with embedded QDs. Moreover, we observed no traces of QDs which could be extracted from the composite into the solvent.

As mentioned above, to test the photostability of CZIS QDs in cross-linked PIB-MA matrices, we prepared composites of the same QDs with two different polymers. The first reference sample was the composite of PIB-SH-capped CZIS QDs in SIBS (M_n = 30 000 g mol^{-1} and M_w/M_n = 1.7 (M_n of PIB block = 21 000 g mol^{-1} and M_w/M_n = 1.2)). As expected, we observed an excellent compatibility between PIB-SH-modified QDs and SIBS. The second reference sample was the composite of pentane/dodecane thiol-treated CZIS QDs in PLMA (M_n = 236 000 g mol^{-1} and M_w/M_n = 2.2). PLMA is a widely used polymer for fabrication of transparent composites with hydrophobic QDs due to interaction of lauryl-groups of the polymer with alkyl chains of the QDs ligands.[61] To correctly compare different composites we used the same conditions for their preparation, including the parameters of film deposition. All obtained composites were transparent films without phase separation, retaining bright PL under the UV-light excitation (see Fig. 3a).

In Fig. 3b the absorption and PL spectra of composites of CZIS QDs with various polymers are displayed. Comparing the spectra one can see that they are practically not altered after

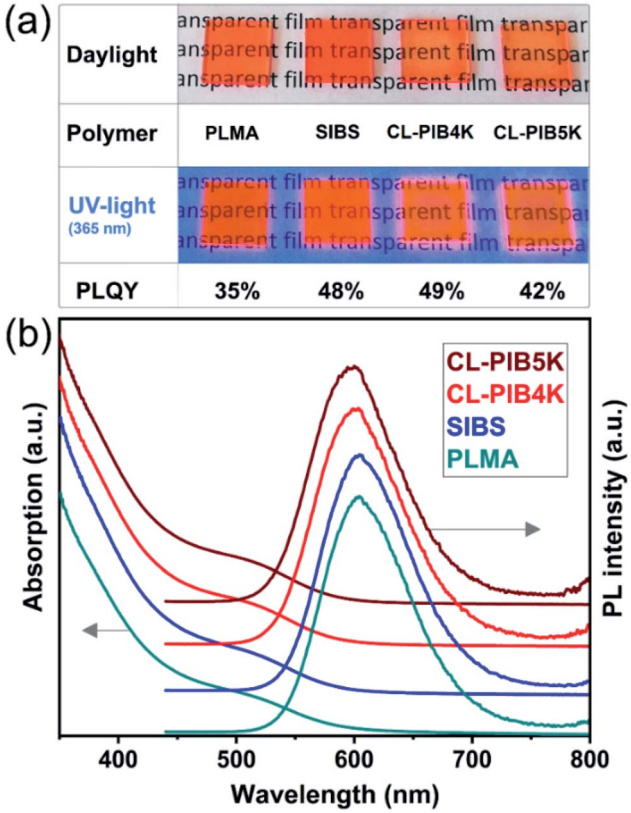

Fig. 3 Photographs of the composites of CZIS QDs in various polymer matrices and corresponding values of their PLQYs (a). Absorption and PL spectra of CZIS QDs-in-polymer composites (b). The spectra are offset vertically for clarity.

incorporating the QDs in solid films, which reveals perfect compatibility between the particles and the matrices achieved by means of the surface engineering. The absorption spectra show no scattering that is proof of the absence of large QD aggregates in all the composites studied. Although we assume the absence of large QD aggregates following from the results of optical spectroscopy, we cannot exclude the formation of small clusters containing a few particles in the film. This clustering typically results in PL quenching due to efficient energy/charge transfer between adjacent QDs observed in 3D networks.[62,63] Our results, however, show that the whole incorporation process of CZIS QDs into CL-PIB4K led to only a slight decrease of PLQY from 52% to 49%, which is another indirect evidence of a homogeneous distribution of the particles in the matrix without formation of aggregates. Based on these observations we may conclude that fast cross-linking of PIB-MA leads to the formation of transparent solid films with a uniform dispersion of QDs. According to our estimations (details are provided in the ESI†), the cross-linked CL-PIB4K matrix has voids of size comparable to the size of a PIB-SH-capped QD, which results in perfect accommodation of the particles in the polymer. This is achieved owing to a strong interaction between the PIB-capped QDs and the matrix preventing phase separation. Furthermore, as shown previously, the cross-linking of the polymer reduces aggregation of QDs during the matrix formation due to kinetically entrapping the QDs between cross-linking polymer chains.[64] In this way the polymer network surrounds nanocrystals and prevents their aggregation. Larger cell size in the cross-linked CL-PIB5K might be responsible for a slight decrease of the PLQY of the composite to 42% due to formation of small aggregates including several nanoparticles. At the same time, in the case of PLMA, we observed a more pronounced PL quenching (PLQY of 35%), because the linear polymer has no possibility of efficient mechanical trapping of QDs that leads to the formation of small aggregates in between polymer chains. This aggregation is most probably caused by still imperfect compatibility between the ligand shell and the polymer. The high value of the PLQY of QDs-in-SIBS composite (48%) comparable with that of CL-PIB4K-based composite is related to excellent compatibility of the polymer with PIB-SH functionalized QDs. In this case, the van der Waals forces between oligomeric PIB-chains grafted on the QDs surface and PIB units of SIBS are much stronger than in the case of QDs-in-PLMA composite, resulting in a decreased mobility of QDs, which prevents their aggregation. In addition to this, the presence of a bulky ligand more efficiently protects the QDs surface from interaction with oxygen and moisture due to steric hindrances leading to the PLQY increase.[65]

To test the encapsulation properties of cross-linked PIB-MA matrices in comparison with other polymer materials, we have investigated the photostability, including measurements in air and under vacuum to explore the influence of the gas permeability and chemical stability of the matrices. To conduct a reliable test of the sample photodegradation, we made a specially designed setup where the samples were excited at very high intensities using a helium cadmium laser. This provided an accelerated aging environment where the decaying PL output of the sample could be measured over time to ensure a clear comparison between the degradation rates of different samples. Samples could be measured in air or under high vacuum ($\sim 10^{-6}$ mbar) to observe the role of atmosphere in the degradation.

Fig. 4 displays change of integrated PL signal of the composites of CZIS QDs in various polymers as a function of time under high intensity photoexcitation in vacuum and in air. As one can see, CZIS QDs in PIB-based matrices demonstrate significantly enhanced photostability in comparison with QDs embedded in PLMA. Among PIB-based matrices, CL-PIB4K exhibited the best photostability. We attribute this to the star-shaped PIB-MA with smaller molecular weight having smaller arms and therefore forming a denser cross-linked polymer network. The higher cross-linking density decreases permeability to gas and moisture and so improves the stability of the composite. With increasing molecular weight of PIB-MA the gas permeability of the cross-linked matrix increases until it becomes comparable to the linear polymer. This assumption can explain the similar behavior of QDs-in-CL-PIB5K and -SIBS upon testing their photostability in the air. In vacuum we observed different behavior of the PL intensity under laser irradiation. First, as one can see from Fig. 4, the PL intensity increased for all samples during the first minutes of the irradiation. We assume that this effect can be related to accelerated

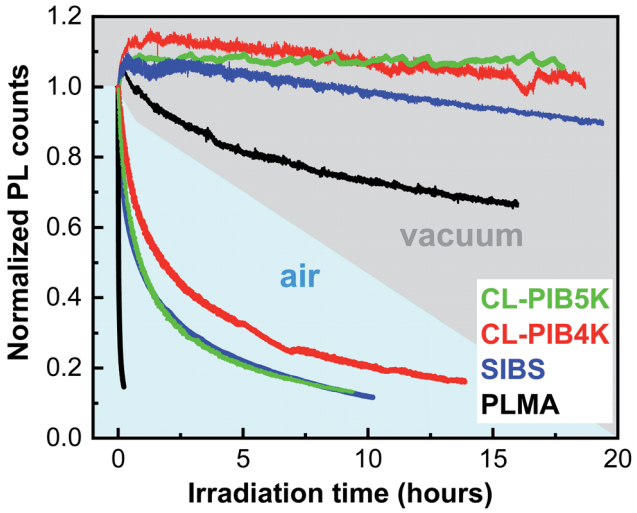

Fig. 4 Normalized PL signal of CZIS QDs-in-polymer composites under air and under vacuum *versus* irradiation time with 42 mW helium–cadmium laser (442 nm).

desorption of water, oxygen, and other low molecular products from the QDs surface under high vacuum and laser treatment. The test of photostability in vacuum allows us to estimate the influence of chemical resistance of the matrix on the degradation of the PL signal of CZIS QDs. As a first approximation, we associate the chemical stability of the matrix with the number of methacrylate groups per unit volume of the polymer. It is known that photodegradation of poly(alkyl methacrylates) results in the photolysis of ester groups accompanied by the formation of free radicals[66,67] which can damage QDs leading to PL quenching. In addition, as can be seen from Fig. 4, the photostability of PLMA-based composites in air is much worse than the PIB-based ones. This can be understood in terms of the low air permeability of the PIB matrices protecting the QDs from photo-oxidation.

An additional test of encapsulating ability of the polymers was soaking of the composites in a concentrated solution of hydrochloric acid, the results of which are displayed in Fig. 5. As in the case of the photostability test, composites of QDs-in-PLMA and -SIBS were assigned as the reference samples. To determine the chemical resistance of the composites, photos of the samples under a UV-lamp were taken during soaking at appropriate time intervals. As can be seen in Fig. 5, PIB-based composites demonstrate excellent resistance of the encapsulated QDs to strong acid in comparison to QDs-in-PLMA composite. Encapsulation properties of polymer matrices are related to their chemical stability and low molecular substance permeability. The results obtained correlate well with the photostability test in air (see Fig. 4), where CL-PIB4K also demonstrated the best result. Thus, the matrices with higher cross-linking density impart better photo- and chemical stability to embedded QDs. Among them, cross-linked PIB-based matrices are one of the best existing options to produce flexible and robust QDs-in-polymer composites resistant to degradation in different media.

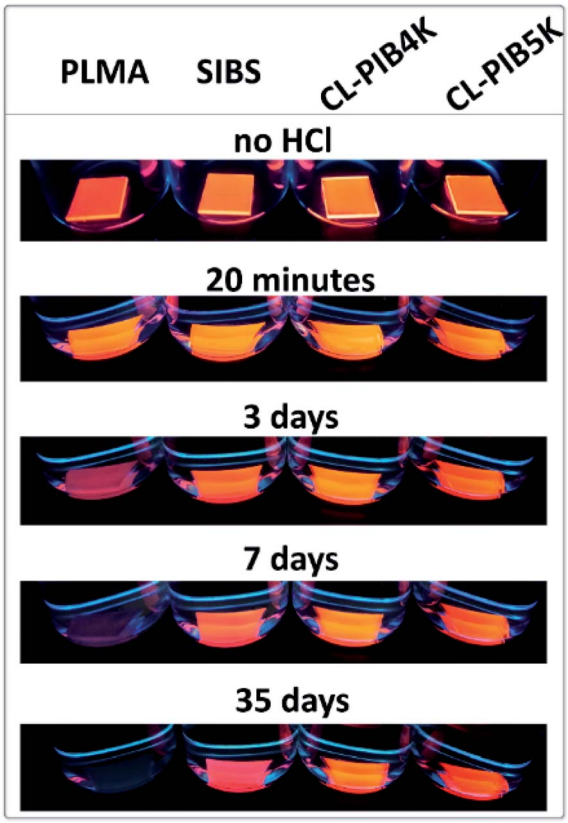

Fig. 5 Photographs of the composites of CZIS QDs-in-polymers taken under UV-light before and after the addition of 5 M solution of HCl. Some distortions in the photos are related to the lens effect of the glass vials filled with HCl solution.

Conclusions

In this work, we developed a promising method for uniform incorporation of colloidal Cd-free QDs into a flexible cross-linked PIB matrix which provides excellent encapsulation to the embedded QDs. We designed the synthesis of a methacrylate-terminated three-arm star-shaped PIB capable of forming a cross-linked polymer network upon UV-light treatment. Owing to the procedure developed of grafting the PIB chains onto the CZIS QDs we achieved uniform dispersion of the QDs in the cross-linked matrix. This enabled the incorporation of the QDs in the polymer matrix without losing their PLQY. Due to the low gas permeability and high chemical stability of the designed cross-linked PIB matrix, the embedded CZIS QDs demonstrated excellent photostability during irradiation of the composite by a powerful 442 nm helium–cadmium laser and high chemical resistance against concentrated acid. The approach developed is a great step forward to creation of durable transparent light conversion films for luminescent solar concentrators, color-conversion LEDs, laser diodes, *etc.*

Author contributions

The manuscript was written through contributions of all authors. All authors have given approval to the final version of the manuscript.

Conflicts of interest

The authors declare no competing financial interest.

Acknowledgements

This work was supported by the EU Horizon 2020 Project MiLEDi (779373) and by the Belarusian Republican Foundation for Fundamental Research (grant X21MC-007). We are grateful to S. Goldberg (TU Dresden) for TEM imaging. D. I. Shiman, E. Ksendzov, E. A. Bolotina, and S. V. Kostjuk acknowledge the support by the Erasmus+ Traineeship Programme for Higher Education.

References

1 A. M. Smith and S. Nie, Semiconductor Nanocrystals: Structure, Properties, and Band Gap Engineering, *Acc. Chem. Res.*, 2010, **43**, 190–200.
2 A. K. Srivastava, W. Zhang, J. Schneider, J. E. Halpert and A. L. Rogach, Luminescent Down-Conversion Semiconductor Quantum Dots and Aligned Quantum Rods for Liquid Crystal Displays, *Adv. Sci.*, 2019, **6**, 1901345.
3 B. Xie, R. Hu and X. Luo, Quantum Dots-Converted Light-Emitting Diodes Packaging for Lighting and Display: Status and Perspectives, *J. Electron. Packag.*, 2016, **138**, 020803.
4 J. Ziegler, S. Xu, E. Kucur, F. Meister, M. Batentschuk, F. Gindele and T. Nann, Silica-Coated InP/ZnS Nanocrystals as Converter Material in White LEDs, *Adv. Mater.*, 2008, **20**, 4068–4073.
5 C. Yoon, T. Kim, M.-H. Shin, Y.-G. Song, K. Shin, Y.-J. Kim and K. Lee, Highly Luminescent and Stable White Light-Emitting Diodes Created by Direct Incorporation of Cd-Free Quantum Dots in Silicone Resins Using the Thiol Group, *J. Mater. Chem. C*, 2015, **3**, 6908–6915.
6 J. Roh, Y.-S. Park, J. Lim and V. I. Klimov, Optically Pumped Colloidal-Quantum-Dot Lasing in LED-like Devices with an Integrated Optical Cavity, *Nat. Commun.*, 2020, **11**, 271.
7 X. Dai, Y. Deng, X. Peng and Y. Jin, Quantum-Dot Light-Emitting Diodes for Large-Area Displays: Towards the Dawn of Commercialization, *Adv. Mater.*, 2017, **29**, 1607022.
8 G. H. Carey, A. L. Abdelhady, Z. Ning, S. M. Thon, O. M. Bakr and E. H. Sargent, Colloidal Quantum Dot Solar Cells, *Chem. Rev.*, 2015, **115**, 12732–12763.
9 Y. Zhou, H. Zhao, D. Ma and F. Rosei, Harnessing the Properties of Colloidal Quantum Dots in Luminescent Solar Concentrators, *Chem. Soc. Rev.*, 2018, **47**, 5866–5890.
10 F. Li, X. Wang, Z. Xia, C. Pan and Q. Liu, Photoluminescence Tuning in Stretchable PDMS Film Grafted Doped Core/Multishell Quantum Dots for Anticounterfeiting, *Adv. Funct. Mater.*, 2017, **27**, 1700051.
11 X. Qian, Z. Cai, M. Su, F. Li, W. Fang, Y. Li, X. Zhou, Q. Li, X. Feng, W. Li, X. Hu, X. Wang, C. Pan and Y. Song, Printable Skin-Driven Mechanoluminescence Devices via Nanodoped Matrix Modification, *Adv. Mater.*, 2018, **30**, 1800291.
12 T. Otto, M. Müller, P. Mundra, V. Lesnyak, H. V. Demir, N. Gaponik and A. Eychmüller, Colloidal Nanocrystals Embedded in Macrocrystals: Robustness, Photostability, and Color Purity, *Nano Lett.*, 2012, **12**, 5348–5354.
13 M. Adam, T. Erdem, G. M. Stachowski, Z. Soran-Erdem, J. F. L. Lox, C. Bauer, J. Poppe, H. V. Demir, N. Gaponik and A. Eychmüller, Implementation of High-Quality Warm-White Light-Emitting Diodes by a Model-Experimental Feedback Approach Using Quantum Dot–Salt Mixed Crystals, *ACS Appl. Mater. Interfaces*, 2015, **7**, 23364–23371.
14 M. Adam, Z. Wang, A. Dubavik, G. M. Stachowski, C. Meerbach, Z. Soran-Erdem, C. Rengers, H. V. Demir, N. Gaponik and A. Eychmüller, Liquid-Liquid Diffusion-Assisted Crystallization: A Fast and Versatile Approach Toward High Quality Mixed Quantum Dot-Salt Crystals, *Adv. Funct. Mater.*, 2015, **25**, 2638–2645.
15 A. Benad, C. Guhrenz, C. Bauer, F. Eichler, M. Adam, C. Ziegler, N. Gaponik and A. Eychmüller, Cold Flow as Versatile Approach for Stable and Highly Luminescent Quantum Dot–Salt Composites, *ACS Appl. Mater. Interfaces*, 2016, **8**, 21570–21575.
16 J. F. L. Lox, F. Eichler, T. Erdem, M. Adam, N. Gaponik, H. V. Demir, V. Lesnyak and A. Eychmüller, Brightly Luminescent Cu-Zn-In-S/ZnS Core/Shell Quantum Dots in Salt Matrices, *Z. Phys. Chem.*, 2018, **233**, 23–40.
17 S. Jun, J. Lee and E. Jang, Highly Luminescent and Photostable Quantum Dot-Silica Monolith and Its Application to Light-Emitting Diodes, *ACS Nano*, 2013, **7**, 1472–1477.
18 E. Frolova, T. Otto, N. Gaponik and V. Lesnyak, Incorporation of CdTe Nanocrystals into Metal Oxide Matrices Towards Inorganic Nanocomposite Materials, *Z. Phys. Chem.*, 2018, **232**, 1335–1352.
19 K.-H. Haas and H. Wolter, Synthesis, Properties and Applications of Inorganic–Organic Copolymers (ORMOCER®s), *Curr. Opin. Solid State Mater. Sci.*, 1999, **4**, 571–580.
20 G. Schottner, Hybrid Sol–Gel-Derived Polymers: Applications of Multifunctional Materials, *Chem. Mater.*, 2001, **13**, 3422–3435.
21 H. Kim and S. Yang, Responsive Smart Windows from Nanoparticle–Polymer Composites, *Adv. Funct. Mater.*, 2020, **30**, 1902597.
22 J. Loste, J. M. Lopez-Cuesta, L. Billon, H. Garay and M. Save, Transparent Polymer Nanocomposites: An Overview on Their Synthesis and Advanced Properties, *Prog. Polym. Sci.*, 2019, **89**, 133–158.
23 W. Cha, H.-J. Kim, S. Lee and J. Kim, Size-Controllable and Stable Organometallic Halide Perovskite Quantum Dots/Polymer Films, *J. Mater. Chem. C*, 2017, **5**, 6667–6671.
24 R. Lesyuk, B. Cai, U. Reuter, N. Gaponik, D. Popovych and V. Lesnyak, Quantum-Dot-in-Polymer Composites via Advanced Surface Engineering, *Small Methods*, 2017, **1**, 1700189.
25 M. Tamborra, M. Striccoli, R. Comparelli, M. L. Curri, A. Petrella and A. Agostiano, Optical Properties of Hybrid Composites Based on Highly Luminescent CdS

Nanocrystals in Polymer, *Nanotechnology*, 2004, **15**, S240–S244.

26 S. V. Kostjuk, H. Y. Yeong and B. Voit, Cationic Polymerization of Isobutylene at Room Temperature, *J. Polym. Sci., Part A: Polym. Chem.*, 2013, **51**, 471–486.

27 D. I. Shiman, V. Sayevich, C. Meerbach, P. A. Nikishau, I. V. Vasilenko, N. Gaponik, S. V. Kostjuk and V. Lesnyak, Robust Polymer Matrix Based on Isobutylene (Co)Polymers for Efficient Encapsulation of Colloidal Semiconductor Nanocrystals, *ACS Appl. Nano Mater.*, 2019, **2**, 956–963.

28 P. D. Cunningham, J. B. Souza, I. Fedin, C. She, B. Lee and D. V. Talapin, Assessment of Anisotropic Semiconductor Nanorod and Nanoplatelet Heterostructures with Polarized Emission for Liquid Crystal Display Technology, *ACS Nano*, 2016, **10**, 5769–5781.

29 N. Tomczak, D. Jańczewski, M. Han and G. J. Vancso, Designer Polymer-Quantum Dot Architectures, *Prog. Polym. Sci.*, 2009, **34**, 393–430.

30 T. Rath, M. Edler, W. Haas, A. Fischereder, S. Moscher, A. Schenk, R. Trattnig, M. Sezen, G. Mauthner, A. Pein, D. Meischler, K. Bartl, R. Saf, N. Bansal, S. A. Haque, F. Hofer, E. J. W. List and G. Trimmel, A Direct Route Towards Polymer/Copper Indium Sulfide Nanocomposite Solar Cells, *Adv. Energy Mater.*, 2011, **1**, 1046–1050.

31 D. Fragouli, A. M. Laera, P. P. Pompa, G. Caputo, V. Resta, M. Allione, L. Tapfer, R. Cingolani and A. Athanassiou, Localized Formation and Size Tuning of CdS Nanocrystals upon Irradiation of Metal Precursors Embedded in Polymer Matrices, *Microelectron. Eng.*, 2009, **86**, 816–819.

32 F. Antolini and L. Orazi, Quantum Dots Synthesis Through Direct Laser Patterning: A Review, *Front. Chem.*, 2019, **7**, 252.

33 C. de M. Donegá, Synthesis and Properties of Colloidal Heteronanocrystals, *Chem. Soc. Rev.*, 2011, **40**, 1512–1546.

34 M.-Q. Dai and L.-Y. L. Yung, Ethylenediamine-Assisted Ligand Exchange and Phase Transfer of Oleophilic Quantum Dots: Stripping of Original Ligands and Preservation of Photoluminescence, *Chem. Mater.*, 2013, **25**, 2193–2201.

35 H. Moon, C. Lee, W. Lee, J. Kim and H. Chae, Stability of Quantum Dots, Quantum Dot Films, and Quantum Dot Light-Emitting Diodes for Display Applications, *Adv. Mater.*, 2019, **31**, 1804294.

36 L. Li, T. J. Daou, I. Texier, T. T. Kim Chi, N. Q. Liem and P. Reiss, Highly Luminescent $CuInS_2$/ZnS Core/Shell Nanocrystals: Cadmium-Free Quantum Dots for In Vivo Imaging, *Chem. Mater.*, 2009, **21**, 2422–2429.

37 A. C. Berends, W. van der Stam, J. P. Hofmann, E. Bladt, J. D. Meeldijk, S. Bals and C. de Mello Donega, Interplay between Surface Chemistry, Precursor Reactivity, and Temperature Determines Outcome of ZnS Shelling Reactions on $CuInS_2$ Nanocrystals, *Chem. Mater.*, 2018, **30**, 2400–2413.

38 K. Gong and D. F. Kelley, Lattice Strain Limit for Uniform Shell Deposition in Zincblende CdSe/CdS Quantum Dots, *J. Phys. Chem. Lett.*, 2015, **6**, 1559–1562.

39 L. M. Robeson, Polymer Membranes for Gas Separation, *Curr. Opin. Solid State Mater. Sci.*, 1999, **4**, 549–552.

40 L. McKeen, *Permeability Properties of Plastics and Elastomers*, Elsevier, 2012.

41 P. Le Floch, S. Meixuanzi, J. Tang, J. Liu and Z. Suo, Stretchable Seal, *ACS Appl. Mater. Interfaces*, 2018, **10**, 27333–27343.

42 B. Yang, C. M. Parada and R. F. Storey, Synthesis, Characterization, and Photopolymerization of Polyisobutylene Phenol (Meth)Acrylate Macromers, *Macromolecules*, 2016, **49**, 6173–6185.

43 S. Banerjee, R. Tripathy, D. Cozzens, T. Nagy, S. Keki, M. Zsuga and R. Faust, Photoinduced Smart, Self-Healing Polymer Sealant for Photovoltaics, *ACS Appl. Mater. Interfaces*, 2015, **7**, 2064–2072.

44 M. Bag, S. Banerjee, R. Faust and D. Venkataraman, Self-Healing Polymer Sealant for Encapsulating Flexible Solar Cells, *Sol. Energy Mater. Sol. Cells*, 2016, **145**, 418–422.

45 D. Chouikhi, I. Kulai, D. Bergbreiter, M. Al-Hashimi and H. Bazzi, Functionalized Polyisobutylene and Liquid/Liquid Separations as a Method for Scavenging Transition Metals from Homogeneously Catalyzed Reactions, *Appl. Sci.*, 2018, **9**, 120.

46 R. F. Storey and Y. Lee, Living Carbocationic Polymerization of Isobutylene Using Blocked Dicumyl Chloride or Tricumyl Chloride/$TiCl_4$ Pyridine Initiating System, *J. Macromol. Sci., Part A: Pure Appl.Chem.*, 1992, **29**, 1017–1030.

47 E. L. Malins, C. Waterson and C. R. Becer, Controlled Synthesis of Amphiphilic Block Copolymers Based on Poly(Isobutylene) Macromonomers, *J. Polym. Sci., Part A: Polym. Chem.*, 2016, **54**, 634–643.

48 L. Yang, A. Antanovich, A. Prudnikau, O. S. Taniya, K. V. Grzhegorzhevskii, P. Zelenovskiy, T. Terpinskaya, J. Tang and M. Artemyev, Highly Luminescent Zn–Cu–In–S/ZnS Core/Gradient Shell Quantum Dots Prepared from Indium Sulfide by Cation Exchange for Cell Labeling and Polymer Composites, *Nanotechnology*, 2019, **30**, 395603.

49 P.-F. Yan, A.-R. Guo, Q. Liu and Y.-X. Wu, Living Cationic Polymerization of Isobutylene Coinitiated by $FeCl_3$ in the Presence of Isopropanol, *J. Polym. Sci., Part A: Polym. Chem.*, 2012, **50**, 3383–3392.

50 A.-R. Guo, X.-J. Yang, P.-F. Yan and Y.-X. Wu, Synthesis of Highly Reactive Polyisobutylenes with Exo-Olefin Terminals via Controlled Cationic Polymerization with $H_2O/FeCl_3$/*i*-PrOH Initiating System in Nonpolar Hydrocarbon Media, *J. Polym. Sci., Part A: Polym. Chem.*, 2013, **51**, 4200–4212.

51 S. Ehlert, C. Stegelmeier, D. Pirner and S. Förster, A General Route to Optically Transparent Highly Filled Polymer Nanocomposites, *Macromolecules*, 2015, **48**, 5323–5327.

52 D. Moodelly, P. Kowalik, P. Bujak, A. Pron and P. Reiss, Synthesis, Photophysical Properties and Surface Chemistry of Chalcopyrite-Type Semiconductor Nanocrystals, *J. Mater. Chem. C*, 2019, **7**, 11665–11709.

53 J. Zhang, R. Xie and W. Yang, A Simple Route for Highly Luminescent Quaternary Cu-Zn-In-S Nanocrystal Emitters, *Chem. Mater.*, 2011, **23**, 3357–3361.

54 Y.-H. Won, O. Cho, T. Kim, D.-Y. Chung, T. Kim, H. Chung, H. Jang, J. Lee, D. Kim and E. Jang, Highly Efficient and

Stable InP/ZnSe/ZnS Quantum Dot Light-Emitting Diodes, *Nature*, 2019, **575**, 634–638.

55 B. Huang, R. Xu, L. Zhang, Y. Yuan, C. Lu, Y. Cui and J. Zhang, Effect of Cu/In Ratio and Shell Thickness on the Photo-Stability of $CuInS_2$/ZnS Nanocrystals, *J. Mater. Chem. C*, 2017, **5**, 12151–12156.

56 O. Yarema, M. Yarema and V. Wood, Tuning the Composition of Multicomponent Semiconductor Nanocrystals: The Case of I-III-VI Materials, *Chem. Mater.*, 2018, **30**, 1446–1461.

57 A. Lefrançois, B. Luszczynska, B. Pepin-Donat, C. Lombard, B. Bouthinon, J.-M. Verilhac, M. Gromova, J. Faure-Vincent, S. Pouget, F. Chandezon, S. Sadki and P. Reiss, Enhanced Charge Separation in Ternary P3HT/PCBM/$CuInS_2$ Nanocrystals Hybrid Solar Cells, *Sci. Rep.*, 2015, **5**, 7768.

58 A. Antanovich, A. Prudnikau, A. Matsukovich, A. Achtstein and M. Artemyev, Self-Assembly of CdSe Nanoplatelets into Stacks of Controlled Size Induced by Ligand Exchange, *J. Phys. Chem. C*, 2016, **120**, 5764–5775.

59 J. S. Owen, J. Park, P.-E. Trudeau and A. P. Alivisatos, Reaction Chemistry and Ligand Exchange at Cadmium−Selenide Nanocrystal Surfaces, *J. Am. Chem. Soc.*, 2008, **130**, 12279–12281.

60 D. Lin-Vien, N. B. Colthup, W. G. Fateley and J. G. Grasselli, *The Handbook of Infrared and Raman Characteristic Frequencies of Organic Molecules*, Academic Press, San Diego, 1991.

61 J. Lee, V. C. Sundar, J. R. Heine, M. G. Bawendi and K. F. Jensen, Full Color Emission from II-VI Semiconductor Quantum Dot-Polymer Composites, *Adv. Mater.*, 2000, **12**, 1102–1105.

62 V. Lesnyak, A. Wolf, A. Dubavik, L. Borchardt, S. V. Voitekhovich, N. Gaponik, S. Kaskel and A. Eychmüller, 3D Assembly of Semiconductor and Metal Nanocrystals: Hybrid CdTe/Au Structures with Controlled Content, *J. Am. Chem. Soc.*, 2011, **133**, 13413–13420.

63 A. Wolf, V. Lesnyak, N. Gaponik and A. Eychmüller, Quantum-Dot-Based (Aero)Gels: Control of the Optical Properties, *J. Phys. Chem. Lett.*, 2012, **3**, 2188–2193.

64 S. V. Vaidya, A. Couzis and C. Maldarelli, Reduction in Aggregation and Energy Transfer of Quantum Dots Incorporated in Polystyrene Beads by Kinetic Entrapment Due to Cross-Linking during Polymerization, *Langmuir*, 2015, **31**, 3167–3179.

65 S. Kim and M. G. Bawendi, Oligomeric Ligands for Luminescent and Stable Nanocrystal Quantum Dots, *J. Am. Chem. Soc.*, 2003, **125**, 14652–14653.

66 R. B. Fox, L. G. Isaacs and S. Stokes, Photolytic Degradation of Poly(Methyl Methacrylate), *J. Polym. Sci., Part A: Gen. Pap.*, 1963, **1**, 1079–1086.

67 G. Geuskens, Photodegradation of Polymers, in *Degradation of Polymers, Comprehensive Chemical Kinetics*, ed. C. H. Bamford and C. F. H. Tipper, Elsevier, 1975, Ch. 3, vol. 14, pp. 333–424.